



## Promoting effect of $\text{MoO}_3$ on the $\text{NO}_x$ reduction by $\text{NH}_3$ over $\text{CeO}_2/\text{TiO}_2$ catalyst studied with in situ DRIFTS

Zhiming Liu<sup>a,\*</sup>, Shaoxuan Zhang<sup>a</sup>, Junhua Li<sup>b</sup>, Lingling Ma<sup>c</sup>

<sup>a</sup> State Key Laboratory of Chemical Resource Engineering, Beijing University of Chemical Technology, Beijing 100029, China

<sup>b</sup> School of Environment, Tsinghua University, Beijing 100084, China

<sup>c</sup> Key laboratory of Nuclear Analytical Techniques, Institute of High Energy Physics, Chinese Academy of Sciences, Beijing 100049, China

### ARTICLE INFO

#### Article history:

Received 17 April 2013

Received in revised form 6 June 2013

Accepted 27 June 2013

Available online 8 July 2013

#### Keywords:

Nitrogen oxides

Selective catalytic reduction

CeMoTi

DRIFTS

### ABSTRACT

A series of  $\text{MoO}_3$ -doped  $\text{CeO}_2/\text{TiO}_2$  catalysts prepared by the impregnation method were investigated for the selective catalytic reduction of  $\text{NO}_x$  by  $\text{NH}_3$ ( $\text{NH}_3$ -SCR). It was found that  $\text{CeO}_2\text{-MoO}_3/\text{TiO}_2$  catalyst is much more active than  $\text{CeO}_2/\text{TiO}_2$  for  $\text{NH}_3$ -SCR and the optimum  $\text{MoO}_3$  loading is 5%. The mechanistic cause of the promoting effect of  $\text{MoO}_3$  on the activity of  $\text{CeO}_2/\text{TiO}_2$  catalyst for  $\text{NH}_3$ -SCR was studied using in situ diffuse reflectance infrared transform spectroscopy (DRIFTS). The results revealed that the highly dispersed molybdenum on  $\text{CeO}_2\text{-MoO}_3/\text{TiO}_2$  catalyst not only resulted in more Brønsted acid sites formed on the catalyst surface, but also reduced the thermal stability of the inactive nitrate species, leaving more active sites available for the adsorption of  $\text{NH}_3$ , both of which are favorable for the promotion of SCR activity.

© 2013 Elsevier B.V. All rights reserved.

## 1. Introduction

Nitrogen oxides ( $\text{NO}_x$ ) emitted from mobile and stationary sources are the major air pollutants, as they cause environmental problems such as acid rain, photochemical smog and ozone depletion [1]. Selective catalytic reduction of  $\text{NO}_x$  with  $\text{NH}_3$  ( $\text{NH}_3$ -SCR) is one effective method for abating  $\text{NO}_x$  in the flue gas from stationary source and the most widely used catalyst system for this process is  $\text{V}_2\text{O}_5\text{-WO}_3(\text{MoO}_3)/\text{TiO}_2$  catalyst [2,3]. However, there are still some inevitable problems with this catalyst system including the toxicity of vanadium species, the narrow temperature window of 300–400 °C, the high conversion of  $\text{SO}_2$  to  $\text{SO}_3$  and the low  $\text{N}_2$  selectivity at high temperatures [2,4]. Hence, developing environmentally benign  $\text{NH}_3$ -SCR catalyst with no vanadium but high catalytic performance is desirable.

Recently,  $\text{CeO}_2$  based oxides have attracted increasing attention for their use as  $\text{NH}_3$ -SCR catalysts due to the high oxygen storage capacity and excellent redox property of  $\text{CeO}_2$  [5–9]. Xu et al. [9] reported that  $\text{Ce}/\text{TiO}_2$  catalyst prepared by impregnation method is active for the  $\text{NH}_3$ -SCR of  $\text{NO}_x$ . And the catalyst prepared by sol-gel method showed higher activity than that prepared by impregnation method [10]. The Ce–O–Ti short-range order species with the interaction between Ce and Ti in atomic scale are proposed to be the active sites on the Ce-Ti catalyst by Li et al. [11]. The doping of

tungsten to  $\text{Ce}/\text{TiO}_2$  leads to the enhanced SCR activity due to the strong interaction between Ce and W [12].

Lietti and co-workers found that the structural and morphological characteristics of  $\text{MoO}_3/\text{TiO}_2$  and  $\text{WO}_3/\text{TiO}_2$  are similar, whereas the reactivity was different which may be due to different redox characteristics of the two samples [13,14]. Further studies revealed that the addition of  $\text{WO}_3$  and  $\text{MoO}_3$  to  $\text{V}_2\text{O}_5/\text{TiO}_2$  are similar, and both oxides acting as “chemical” promoters besides playing a “structural” function as well [15,16]. Considering the similarities of  $\text{MoO}_3$  and  $\text{WO}_3$  and the lower price of  $\text{MoO}_3$  [17], the present work attempts to improve the activity of  $\text{Ce}/\text{TiO}_2$  catalyst by adding molybdenum oxide to develop a novel non-vanadium  $\text{NH}_3$ -SCR catalyst with high catalytic activity in a wider temperature window. It was found that the addition of  $\text{MoO}_3$  showed a noticeable promoting effect on the activity of  $\text{Ce}/\text{TiO}_2$  for the  $\text{NH}_3$ -SCR at relatively low temperatures. On the basis of in situ diffuse reflectance infrared transform spectroscopy (DRIFT) experiments the mechanistic cause of the promoting effect was elucidated.

## 2. Experimental

### 2.1. Catalyst preparation

The catalysts were prepared by impregnation method, and Degussa AEROSIL  $\text{TiO}_2$  P25 was used as support. 10 wt.%  $\text{CeO}_2/\text{TiO}_2$  ( $\text{Ce}_{10}\text{Ti}$ ) catalyst was prepared by impregnating  $\text{TiO}_2$  with a proper amount of cerium nitrate ( $\text{Ce}(\text{NO}_3)_3\cdot 6\text{H}_2\text{O}$ ) solution, then stirred for 4 h, followed by drying at 120 °C and calcinations at 500 °C for

\* Corresponding author. Tel.: +86 10 64427356.

E-mail address: [liuzm@mail.buct.edu.cn](mailto:liuzm@mail.buct.edu.cn) (Z. Liu).

4 h in air.  $\text{MoO}_3/\text{TiO}_2$  catalysts with  $\text{MoO}_3$  loading varying from 2–8 wt.% ( $\text{Mo}_x\text{Ti}$ ) were prepared by the same method as described above using ammonium molybdate ( $(\text{NH}_4)_6\text{Mo}_7\text{O}_{24}\cdot 4\text{H}_2\text{O}$ ) and oxalic acid ( $\text{H}_2\text{C}_2\text{O}_4\cdot 2\text{H}_2\text{O}$ ) solution instead.  $\text{Ce}_{10}\text{Mo}_x\text{Ti}$  catalyst was prepared by impregnating  $\text{Mo}_x\text{Ti}$  powder with an aqueous solution of cerium nitrate, stirred for 4 h, then dried at 120 °C and calcined at 500 °C for 4 h in air. For comparison, the state-of-the art SCR  $\text{V}_2\text{O}_5\text{-WO}_3/\text{TiO}_2$  catalyst with 1 wt.%  $\text{V}_2\text{O}_5$  and 5 wt.%  $\text{WO}_3$  was also prepared by the same impregnation method using  $\text{NH}_4\text{VO}_3$ ,  $(\text{NH}_4)_{10}\text{W}_{12}\text{O}_{41}$ ,  $\text{H}_2\text{C}_2\text{O}_4\cdot 2\text{H}_2\text{O}$  as precursors.

## 2.2. Catalytic activity measurement

The activity measurements were carried out in a fixed-bed quartz reactor using a 0.12 g catalyst of 40–60 meshes. The feed gas mixture contained 500 ppm NO, 500 ppm  $\text{NH}_3$ , 5%  $\text{O}_2$  and helium as the balance gas. The total flow rate of the feed gas was  $300\text{ cm}^3\text{ min}^{-1}$ , corresponding to a GHSV of  $128,000\text{ h}^{-1}$ . The reaction temperature was increased from 200 to 450 °C. The composition of the product gas was analyzed by a chemiluminescence NO/NO<sub>2</sub> analyzer (Thermal Scientific, model 42i-HL) and gas chromatograph (Shimadzu GC 2014 equipped with Porapak Q and Molecular sieve 5A columns). The activity data were collected when the catalytic reaction practically reached steady-state condition at each temperature.

## 2.3. Catalyst characterization

Characterization of the BET surface area of the samples was carried out with a Quantachrome Autosorb AS-1 system. Prior to the surface area measurements, the samples were degassed in vacuum at 400 °C for 4 h. Powder X-ray diffraction (XRD) measurements were recorded on a Brucker D8 ADVANCE system with Cu K $\alpha$  radiation at 45 kV and 200 mA. Temperature-programmed reduction ( $\text{H}_2\text{-TPR}$ ) experiments were conducted on a chemisorption analyzer (Micromeritics, ChemiSorb 2720 TPX) under a 10%  $\text{H}_2$  gas flow ( $50\text{ cm}^3\text{ min}^{-1}$ ) at a rate of  $10\text{ }^{\circ}\text{C min}^{-1}$  up to 1000 °C.

In situ DRIFTS spectra were recorded using a thermo Nicolet 6700 spectrometer equipped with a high temperature environmental cell fitted with ZnSe window and an MCT detector cooled with liquid N<sub>2</sub>. The catalyst was loaded in the Harrick IR cell and heated to 400 °C under helium at a total flow rate of  $100\text{ cm}^3\text{ min}^{-1}$  for 60 min to remove adsorbed impurities. A background spectrum was collected under a flowing helium atmosphere and was subtracted from the sample spectra. The DRIFTS spectra were recorded by accumulating 100 scans with a resolution of  $4\text{ cm}^{-1}$ .

## 3. Results and discussion

### 3.1. $\text{NH}_3\text{-SCR}$ activity

$\text{NH}_3\text{-SCR}$  activities of  $\text{CeTi}$ ,  $\text{MoTi}$  and  $\text{CeMoTi}$  catalysts were evaluated as a function of temperature and the results are presented in Fig. 1. It is evident that the addition of 2% Mo to  $\text{Ce}_{10}\text{Ti}$  showed a remarkable promoting effect below 325 °C. With the increasing of  $\text{MoO}_3$  loadings from 2% to 5%,  $\text{NO}_x$  conversion was further increased. Further increasing the Mo loading to 8% leads to a decrease of the activity, but it is still higher than that of  $\text{Ce}_{10}\text{Ti}$  catalyst below 275 °C. Therefore, the optimum loading of  $\text{MoO}_3$  is 5%. For  $\text{Ce}_{10}\text{Mo}_5\text{Ti}$  catalyst, nearly 90% of  $\text{NO}_x$  conversion was obtained in a wide temperature range (275–400 °C) under a high GHSV of  $128,000\text{ h}^{-1}$ . And the  $\text{NO}_x$  conversion starts to decrease when the temperature is higher than 400 °C. Compared with  $\text{Ce}_{10}\text{Ti}$  and  $\text{Mo}_5\text{Ti}$  catalysts,  $\text{Ce}_{10}\text{Mo}_5\text{Ti}$  exhibited much higher activity below 325 °C, indicating that the coexistence of Ce and a proper amount of Mo is very important for the SCR activity.

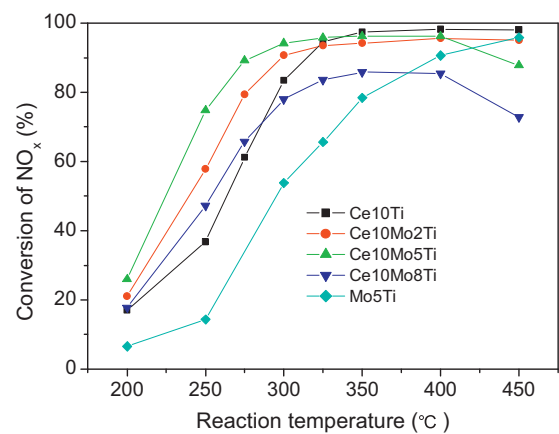


Fig. 1. Activities of  $\text{Ce}_{10}\text{Ti}$ ,  $\text{Mo}_5\text{Ti}$  and  $\text{Ce}_{10}\text{Mo}_x\text{Ti}$  with various Mo loading for the  $\text{NO}_x$  reduction with  $\text{NH}_3$ . Reaction conditions:  $[\text{NO}] = [\text{NH}_3] = 500\text{ ppm}$ ,  $[\text{O}_2] = 5\%$ , GHSV =  $128,000\text{ h}^{-1}$ .

Fig. 2 showed the comparison of the SCR activities of  $\text{Ce}_{10}\text{Mo}_5\text{Ti}$  and  $\text{V}_2\text{O}_5\text{-WO}_3/\text{TiO}_2$  catalysts. It can be seen that  $\text{Ce}_{10}\text{Mo}_5\text{Ti}$  is more active than the conventional  $\text{V}_2\text{O}_5\text{-WO}_3/\text{TiO}_2$  below 325 °C. Therefore, the environmentally benign  $\text{Ce}_{10}\text{Mo}_5\text{Ti}$  catalyst is promising for the control of  $\text{NO}_x$  emitted from stationary source.

### 3.2. BET surface area, XRD and $\text{H}_2\text{-TPR}$

As shown in Table S1, the surface area of  $\text{Ce}_{10}\text{Ti}$  decreased after doping  $\text{MoO}_3$  and  $\text{Ce}_{10}\text{Mo}_8\text{Ti}$  is of the lowest surface area. This is in accordance with the previous report that the BET surface area of the catalyst decreases as the molybdenum loading increases [14,18]. Although the BET surface area of  $\text{Ce}_{10}\text{Mo}_5\text{Ti}$  was lower than that of  $\text{Ce}_{10}\text{Ti}$  catalyst, it exhibited higher  $\text{NH}_3\text{-SCR}$  activity, indicating that some synergistic effect existed between Ce and Mo species and the BET surface area does not play a key role in the SCR reaction.

Fig. 3 showed the XRD patterns of  $\text{TiO}_2$ ,  $\text{Ce}_{10}\text{Ti}$ ,  $\text{Mo}_5\text{Ti}$  and  $\text{Ce}_{10}\text{Mo}_x\text{Ti}$  with different Mo loading. For all the catalysts, the anatase phase (PDF-ICDD21-1272) was the main phase, and only a little rutile phase (PDF-ICDD21-1276) appeared. It is well worthy to note that the peak ascribed to crystalline  $\text{MoO}_3$  phase was absent for  $\text{Ce}_{10}\text{Mo}_x\text{Ti}$  and  $\text{Mo}_5\text{Ti}$  catalysts, indicating that the molybdenum oxide was highly dispersed on the surface of  $\text{TiO}_2$ . A weak peak of cubic  $\text{CeO}_2$  crystallites was observed over  $\text{Ce}_{10}\text{Ti}$  catalyst [11]. The peak ascribed to  $\text{CeO}_2$  becomes more noticeable after the addition of  $\text{MoO}_3$  to  $\text{Ce}_{10}\text{Ti}$  catalyst, indicating that the introduction of Mo

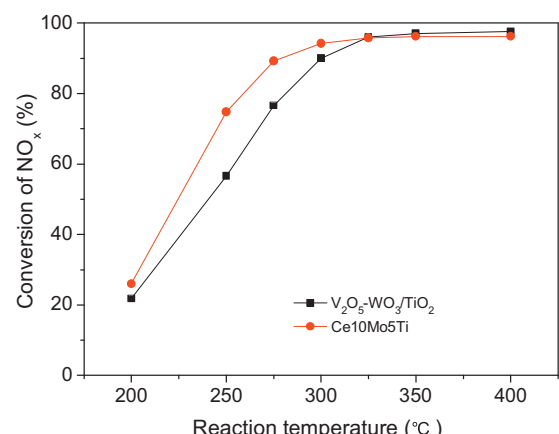
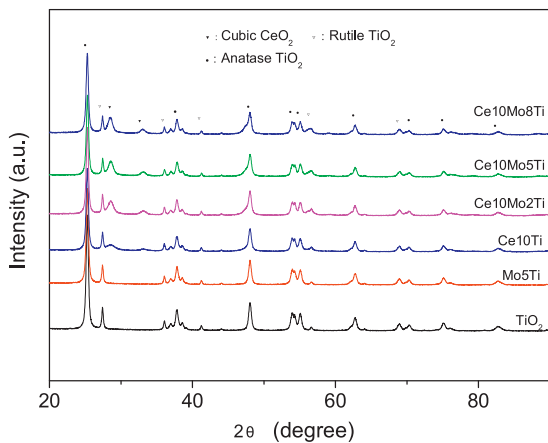


Fig. 2. Comparison of  $\text{NH}_3\text{-SCR}$  activities of  $\text{Ce}_{10}\text{Mo}_5\text{Ti}$  and  $\text{V}_2\text{O}_5\text{-WO}_3/\text{TiO}_2$  catalysts. Reaction conditions:  $[\text{NO}] = [\text{NH}_3] = 500\text{ ppm}$ ,  $[\text{O}_2] = 5\%$ , GHSV =  $128,000\text{ h}^{-1}$ .



**Fig. 3.** XRD patterns of  $\text{TiO}_2$ ,  $\text{Ce}_{10}\text{Ti}$ ,  $\text{Mo}_5\text{Ti}$  and  $\text{Ce}_{10}\text{Mo}_x\text{Ti}$  with different Mo loading.

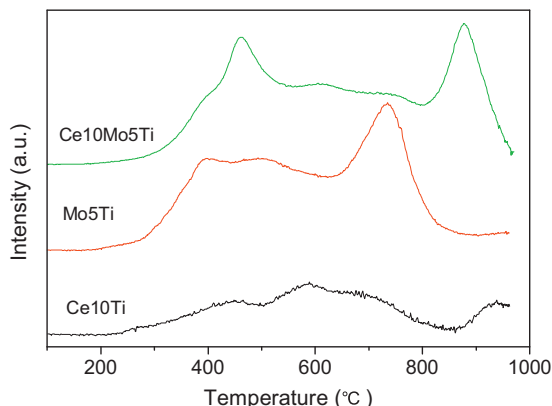
could induce the crystallite of  $\text{CeO}_2$ . The presence of crystallite  $\text{CeO}_2$  could enhance the combustion of  $\text{NH}_3$  with oxygen at high temperatures, thus relatively less  $\text{NH}_3$  remained for the  $\text{NH}_3\text{-SCR}$ , resulting the decrease of  $\text{NO}_x$  conversion (see Fig. 1).

Fig. 4 presents the  $\text{H}_2\text{-TPR}$  profiles on  $\text{Ce}_{10}\text{Ti}$ ,  $\text{Mo}_5\text{Ti}$  and  $\text{Ce}_{10}\text{Mo}_5\text{Ti}$  catalysts. For  $\text{Ce}_{10}\text{Ti}$  catalyst, three reduction peaks centering at 450, 590 and 940  $^\circ\text{C}$  appeared. The two reduction peaks at 450 and 590  $^\circ\text{C}$  can be attributed to the reduction of  $\text{Ce}^{4+}$  to  $\text{Ce}^{3+}$  [19,20], and the peak at 940  $^\circ\text{C}$  might be due to the reduction of bulk  $\text{CeO}_2$  [20].  $\text{Mo}_5\text{Ti}$  also exhibited three reduction peaks at around 400, 500 and 735  $^\circ\text{C}$ . The first two peaks could be assigned to the reduction of the octahedral well dispersed Mo species and the high temperature reduction peak (735  $^\circ\text{C}$ ) could be due to the reduction of tetrahedral Mo species [21], which is in strong interaction with  $\text{TiO}_2$  support. Interestingly,  $\text{Ce}_{10}\text{Mo}_5\text{Ti}$  catalyst possesses two main reduction peaks centering at 460 and 880  $^\circ\text{C}$ . The former one could be assigned to the coreduction of surface  $\text{Ce}^{4+}$  and octahedral well dispersed Mo species, and the latter one is due to the coreduction of bulk  $\text{CeO}_2$  and tetrahedral Mo species. This fact suggests that the synergistic interaction between Ce and Mo exists in  $\text{Ce}_{10}\text{Mo}_5\text{Ti}$  catalyst, which could contribute to the enhanced SCR activity below 325  $^\circ\text{C}$ .

### 3.3. In situ DRIFTS studies

#### 3.3.1. Adsorption of $\text{NH}_3$

Fig. 5(a) showed the DRIFT spectra of  $\text{NH}_3$  adsorption over  $\text{Ce}_{10}\text{Ti}$  catalyst at different temperatures. The bands at 1592 and 1157  $\text{cm}^{-1}$  with shoulder at 1221  $\text{cm}^{-1}$  can be assigned to



**Fig. 4.**  $\text{H}_2\text{-TPR}$  profiles on  $\text{Ce}_{10}\text{Ti}$ ,  $\text{Mo}_5\text{Ti}$  and  $\text{Ce}_{10}\text{Mo}_5\text{Ti}$  catalysts.

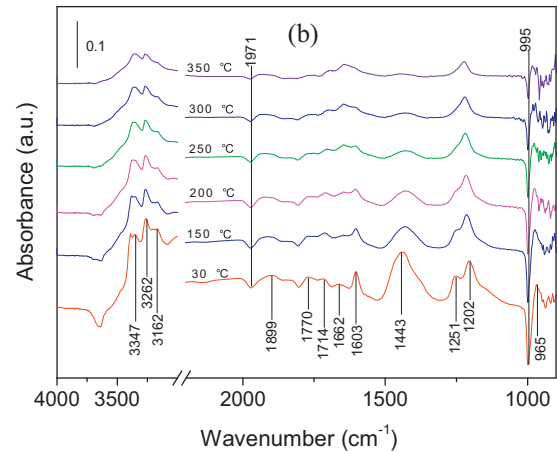
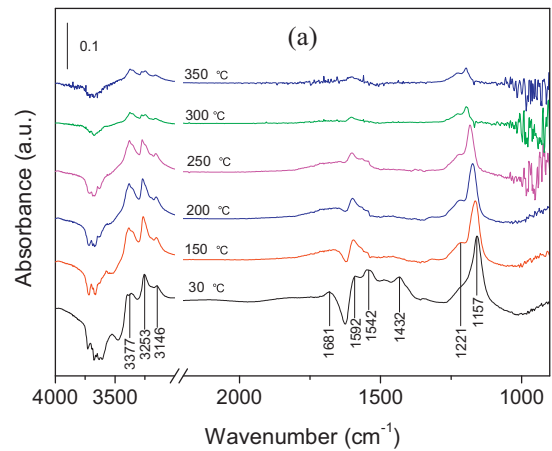


**Fig. 5.** DRIFT spectra of  $\text{Ce}_{10}\text{Ti}$ (a) and  $\text{Ce}_{10}\text{Mo}_5\text{Ti}$ (b) treated in flowing 500 ppm  $\text{NH}_3$  at room temperature for 60 min and then purged by He at 30, 150, 200, 250, 300, and 350  $^\circ\text{C}$ .

asymmetric and symmetric bending vibrations of the coordinated  $\text{NH}_3$  linked to Lewis acid sites [15,22], and that at 3377, 3253 and 3146  $\text{cm}^{-1}$  can be ascribed to the N-H stretching vibration modes of the coordinated  $\text{NH}_3$  [23]. The band at around 1542  $\text{cm}^{-1}$  is ascribed to amid ( $-\text{NH}_2$ ) species [15,23]. The weak bands assigned to asymmetric and symmetric bending vibrations of  $\text{NH}_4^+$  species on Brønsted acid sites (1432 and 1681  $\text{cm}^{-1}$ ) [24,25] were also observed. With increasing temperature, the intensity of the bands assigned to Brønsted acid sites decreased noticeably than that of the bands due to Lewis acid sites. This indicates that ammonia bonded to Lewis acid sites were more stable than that on Brønsted acid sites [26].

As shown in Fig. 5(b), the DRIFT spectra of  $\text{NH}_3$  adsorption over  $\text{Ce}_{10}\text{Mo}_5\text{Ti}$  catalyst were much different from that of  $\text{Ce}_{10}\text{Ti}$  catalyst. Besides the observed coordinated  $\text{NH}_3$  linked to Lewis acid sites (1202, 1251, 1603, 3162, 3262 and 3347  $\text{cm}^{-1}$ ), a new band appeared at 965  $\text{cm}^{-1}$ , which could be assigned to weakly adsorbed or gas phase  $\text{NH}_3$  [27,28]. It is evident that the intensity of the band assigned to Brønsted acid sites (1443  $\text{cm}^{-1}$ ) is much higher than that over  $\text{Ce}_{10}\text{Ti}$  catalyst. Several bands appeared in the range of 1850–1640  $\text{cm}^{-1}$  could also be assigned to  $\text{NH}_4^+$  species on Brønsted acid sites. Whereas only one band appear in this range over  $\text{Ce}_{10}\text{Ti}$  catalyst as described above. These results suggest that the introduction of Mo tremendously increased both the quantity and the intensity of Brønsted acid sites on the catalyst. Previous research showed that Brønsted acid site is beneficial for the adsorption of  $\text{NH}_3$  thus improving the low-temperature activity [26,29]. All the bands decreased with increasing temperature.

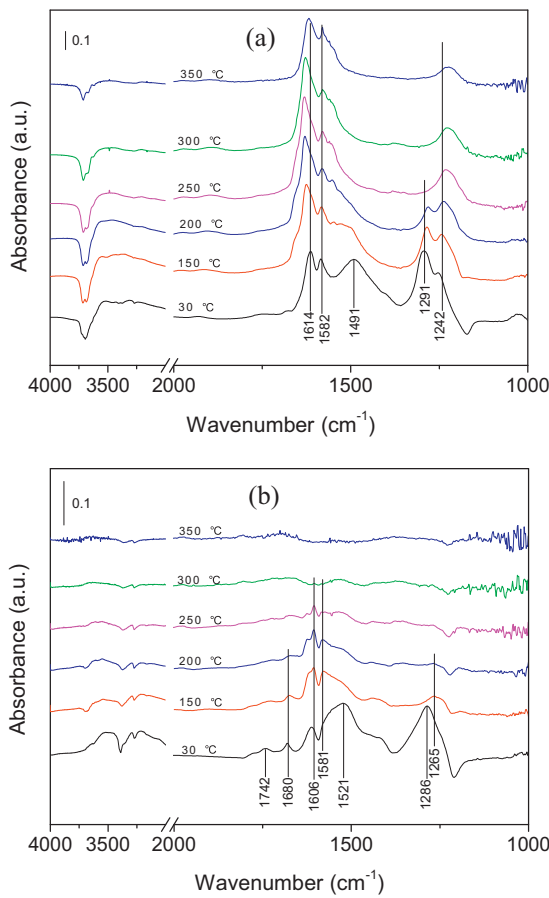


**Fig. 6.** DRIFT spectra of Ce<sub>10</sub>Ti(a) and Ce<sub>10</sub>Mo<sub>5</sub>Ti(b) treated in flowing 500 ppm NO + 5% O<sub>2</sub> at room temperature for 60 min and then purged by He at 30, 150, 200, 250, 300, and 350 °C.

It should be noted that two negative bands around 1000 and 1971 cm<sup>-1</sup> formed over Ce<sub>10</sub>Mo<sub>5</sub>Ti catalyst. The similar bands were also observed over the Mo<sub>5</sub>Ti catalyst (see Fig. S1). Therefore, the negative band is supposed to be due to the molybdenum of the catalyst. Previous study revealed that these two negative bands correspond to the first overtone and the fundamental stretching mode of a single short Mo=O bond of a surface isolated molybdenyl species, respectively [30–32]. This means that molybdenyl species are unsaturated on the catalyst surface and are perturbed by ammonia adsorption, leading to lower Mo=O bond order. Therefore, Molybdenyl species act as adsorption sites for ammonia adsorption, which is in agreement with previous report [23].

### 3.3.2. Co-adsorption of NO and O<sub>2</sub>

The DRIFT spectra of NO + O<sub>2</sub> on Ce<sub>10</sub>Ti catalyst at different temperatures were illustrated in Fig. 6(a). Several distinct bands appeared at 1242, 1291, 1491, 1582 and 1614 cm<sup>-1</sup>, which were respectively assigned to the asymmetric frequency of gaseous NO<sub>2</sub> molecules(1614 cm<sup>-1</sup>) [26], bidentate nitrate(1582 cm<sup>-1</sup>) [33], monodentate nitrate (1291 and 1491 cm<sup>-1</sup>) [34] and bridged nitrate(1242 cm<sup>-1</sup>) [35]. It can be seen that the monodentate nitrate is instable and their intensity decreased with increasing temperature.

Fig. 6(b) showed the DRIFT spectra of NO<sub>x</sub> adsorption over Ce<sub>10</sub>Mo<sub>5</sub>Ti catalyst, which was much different from that of Ce<sub>10</sub>Ti. With the Mo addition, all the bands showed less thermal stability. The bands at 1291 and 1491 cm<sup>-1</sup> ascribed to the instable monodentate nitrate shifted to 1286 and 1521 cm<sup>-1</sup> and appeared only at room temperature. The peaks attributed to

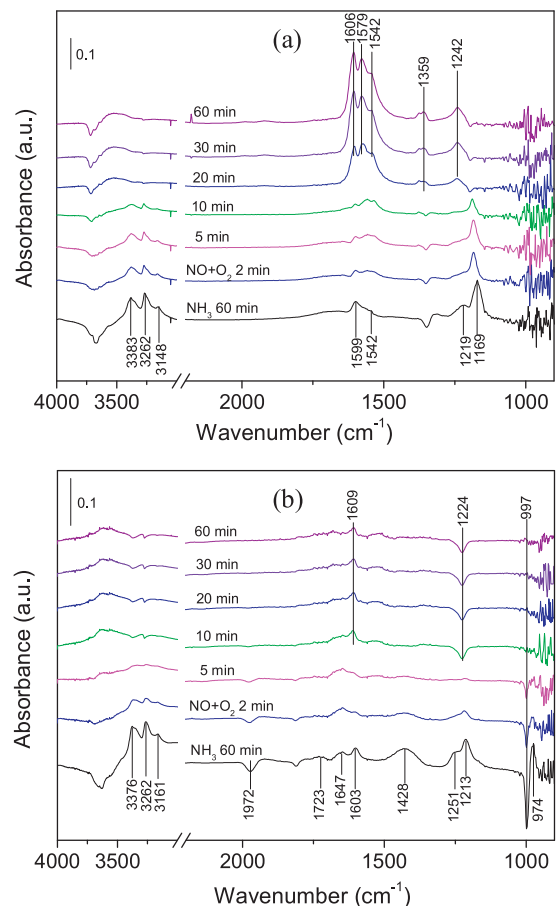


**Fig. 7.** Dynamic changes of the in situ DRIFT spectra over Ce<sub>10</sub>Ti(a) and Ce<sub>10</sub>Mo<sub>5</sub>Ti(b) catalysts as a function of time in a flow of NO + O<sub>2</sub> after the catalysts was pre-exposed to a flow of NH<sub>3</sub> for the 60 min followed by helium purging for 30 min at 250 °C.

bidentate nitrate (1581 cm<sup>-1</sup>) and gaseous NO<sub>2</sub> molecules(1606 cm<sup>-1</sup>) vanished at 250 and 300 °C, respectively. The bridged nitrate species(1242 cm<sup>-1</sup>) was not observed. The two new bands at 1680 and 1742 cm<sup>-1</sup> could be assigned to N<sub>2</sub>O<sub>4</sub> [36] and trans-(NO)<sub>2</sub> [37], respectively. All these results suggest that the addition of Mo significantly reduced the thermal stability of the adsorbed nitrate species and changed their forms as well.

### 3.3.3. Reaction between nitrogen oxides and ammonia adspecies

Fig. 7 showed the DRIFT spectra of Ce<sub>10</sub>Ti and Ce<sub>10</sub>Mo<sub>5</sub>Ti catalysts in a flow of NO + O<sub>2</sub> after the catalysts was pre-exposed to a flow of NH<sub>3</sub> for the 60 min followed by helium purging for 30 min at 250 °C. As shown in Fig. 7 (a), the coordinated NH<sub>3</sub> on Lewis acid sites (1169, 1219 and 1599 cm<sup>-1</sup>) and –NH<sub>2</sub> species (1542 cm<sup>-1</sup>) formed on Ce<sub>10</sub>Ti catalyst with feeding NH<sub>3</sub>. Switching the gas to NO + O<sub>2</sub>, the intensities of all bands assigned to ammonia species decreased and the bands vanished in 10 min. Meanwhile some new bands attributed to NO<sub>x</sub> species (1242, 1542, 1606, 1579 cm<sup>-1</sup>) appeared. The band at 1359 cm<sup>-1</sup> could be assigned to the intermediate species from the combination of surface adsorbed NH<sub>3</sub> and NO<sub>x</sub> species [26].

Compared with Ce<sub>10</sub>Ti, all the bands due to ammonia adspecies and the two negative bands at 997 and 1972 cm<sup>-1</sup> vanished in 2 min after Ce<sub>10</sub>Mo<sub>5</sub>Ti catalyst was purged by NO + O<sub>2</sub>, and subsequently the absorbed NO<sub>2</sub> (1609 cm<sup>-1</sup>) and bridged nitrate (1224 cm<sup>-1</sup>) were observed (see Fig. 7(b)). The band assigned to the combination of surface adsorbed NH<sub>3</sub> and NO<sub>x</sub> species (1359 cm<sup>-1</sup>) is absent. Another interesting phenomenon is that only one band related

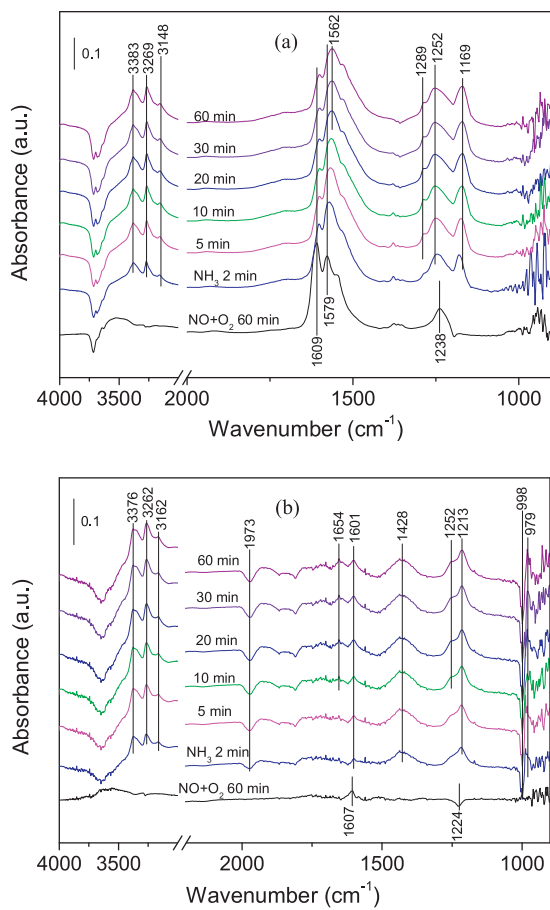


**Fig. 8.** Dynamic changes of the in situ DRIFT spectra over Ce<sub>10</sub>Ti(a) and Ce<sub>10</sub>Mo<sub>5</sub>Ti(b) catalysts as a function of time in a flow of NH<sub>3</sub> after the catalysts was pre-exposed to a flow of NO + O<sub>2</sub> for the 60 min followed by helium purging for 30 min at 250 °C.

to NO<sub>2</sub> appeared, indicating that the adsorption of nitrate species was inhibited. The possible reason is that the addition of MoO<sub>3</sub> to Ce<sub>10</sub>Ti catalyst leads to more acid sites formed with reduced the alkali sites where nitrate species adsorbed. From the comparison between Fig. 7(a) and (b) it can be seen that the adsorbed ammonia species on Ce<sub>10</sub>Mo<sub>5</sub>Ti are more reactive than those on Ce<sub>10</sub>Ti to react with NO<sub>x</sub>, leading to the enhanced SCR activity of NO<sub>x</sub>.

### 3.3.4. Reaction between ammonia and adsorbed nitrogen oxides species

Fig. 8 showed the DRIFT spectra of Ce<sub>10</sub>Ti and Ce<sub>10</sub>Mo<sub>5</sub>Ti catalysts in a flow of NH<sub>3</sub> after the catalysts were pre-exposed to a flow of NO + O<sub>2</sub> for the 60 min followed by N<sub>2</sub> purging for 30 min at 250 °C. As illustrated in Fig. 8 (a), switching the gas to NH<sub>3</sub> leads to an immediate decrease in the intensity of NO<sub>2</sub> peak (1609 cm<sup>-1</sup>). And the peak ascribed to the coordinated NH<sub>3</sub> (1600 and 1169 cm<sup>-1</sup>) with the N–H stretching vibration modes of it (3148, 3269, 3383 cm<sup>-1</sup>) appeared. The peak at 1579 cm<sup>-1</sup> shifted to the lower frequency gradually with feeding NH<sub>3</sub>, which could be the overlap of the NH<sub>2</sub> species and the bidentate nitrate species. The band at 1238 cm<sup>-1</sup> ascribed to the bridging nitrate species transformed to two bands at 1289 and 1252 cm<sup>-1</sup>, both of which might be due to the nitrate species formed by the oxidation of ammonia or the interaction between ammonia and adsorbed NO<sub>x</sub> species [26].

As shown in Fig. 8(b), over Ce<sub>10</sub>Mo<sub>5</sub>Ti catalyst the peak assigned to NO<sub>2</sub> (1606 cm<sup>-1</sup>) diminished in 2 min after NH<sub>3</sub> was introduced into the system. Simultaneously, the peaks ascribed to coordinated NH<sub>3</sub> on Lewis acid sites (3376, 3262, 3162, 1601, 1213 cm<sup>-1</sup> with a shoulder at 1252 cm<sup>-1</sup>) and NH<sub>4</sub><sup>+</sup> species on Brønsted acid sites

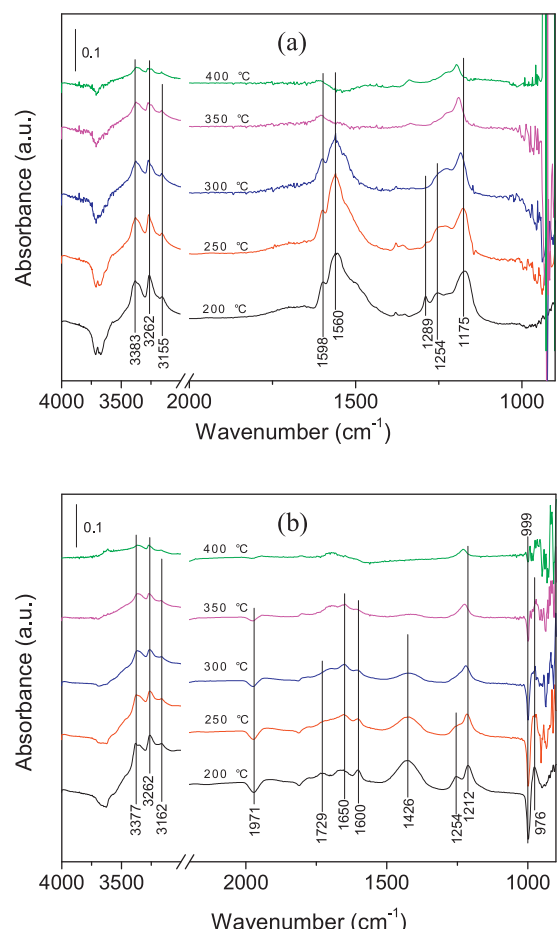


**Fig. 9.** DRIFT spectra of Ce<sub>10</sub>Ti(a) and Ce<sub>10</sub>Mo<sub>5</sub>Ti(b) in a flowing of 500 ppm NH<sub>3</sub> + 500 ppm NO + 5% O<sub>2</sub> at 200, 250, 300, 350 and 400 °C.

(1428 and 1654 cm<sup>-1</sup>) appeared. The band at 965 cm<sup>-1</sup> assigned to weakly adsorbed or gas phase NH<sub>3</sub> were also observed. All the results indicated that the reaction between adsorbed NO<sub>2</sub> and NH<sub>3</sub> easily occurred, especially over Ce<sub>10</sub>Mo<sub>5</sub>Ti catalysts, but the adsorbed nitrate species was unlikely to react with ammonia. With Mo addition, the adsorption of nitrate species was significantly limited as shown in Fig. 6(b), leading to more active sites available for the adsorption and activation of NH<sub>3</sub> thus a higher activity.

### 3.3.5. DRIFT spectra in a flow of NO + NH<sub>3</sub> + O<sub>2</sub>

Fig. 9 showed the in situ DRIFT spectra of Ce<sub>10</sub>Ti and Ce<sub>10</sub>Mo<sub>5</sub>Ti catalysts at various temperatures during the reaction of 500 ppm NH<sub>3</sub>, 500 ppm NO and 5% O<sub>2</sub> under the steady-state condition. On Ce<sub>10</sub>Ti (see Fig. 9(a)) catalyst, bands due to various nitrate species were observed at 1254, 1289, and 1560 cm<sup>-1</sup>. The intensities of these bands are still high until 300 °C, suggesting that the nitrate species were not reactive. Above 300 °C these peaks disappeared quickly. The peaks ascribed to the coordinated NH<sub>3</sub> on Lewis acid sites (3383, 3262, 3155, 1598 and 1175 cm<sup>-1</sup>) were also observed. But the bands due to NH<sub>4</sub><sup>+</sup> species on Brønsted acid sites are absent.

As presented in Fig. 9(b), the DRIFT spectra over Ce<sub>10</sub>Mo<sub>5</sub>Ti are quite different from that over Ce<sub>10</sub>Ti catalyst. No band due to nitrate species was detected in the whole region, which might be caused by the competitive adsorption and followed reactions among NH<sub>3</sub>, NO and O<sub>2</sub>. Different from the adsorption on Ce<sub>10</sub>Ti catalyst, both the coordinated NH<sub>3</sub> on Lewis acid sites (1254 and 1212 cm<sup>-1</sup>) and NH<sub>4</sub><sup>+</sup> species on Brønsted acid sites (1426, 1650 and 1729 cm<sup>-1</sup>) were observed on Ce<sub>10</sub>Mo<sub>5</sub>Ti.

For the NH<sub>3</sub>-SCR process, the Langmuir–Hinshelwood(L-H) and Eley–Rideal (E-R) mechanisms are two of the most accepted mechanism [7,26,38]. From the dynamic changes of the in situ DRIFT spectra of nitrate species after feeding NH<sub>3</sub> over Ce<sub>10</sub>Ti and Ce<sub>10</sub>Mo<sub>5</sub>Ti catalyst (see Fig. 8), it can be seen that the formed nitrate species unlikely participated in the SCR reaction. These generated thermally stable nitrates(NO<sub>3</sub><sup>-</sup>) covered the surface active sites to prohibit the adsorption of NH<sub>3</sub>, thus showing harmful effects for NH<sub>3</sub>-SCR reaction. The similar harmful effect of nitrates was also proposed for cryptomelane-type manganese oxides (OMS-2) catalyst by Sun et al. [39]. For various catalytic systems, different hypotheses have been proposed for the mechanism. However, the adsorption and activation of NH<sub>3</sub> are recognized to be a key step [7,40]. For the Ce<sub>10</sub>Ti catalyst, Lewis acid sites were considered to be the main active sites as shown in Fig. 5(a). NO<sub>2</sub> was also formed as observed in the stable and transient experiment (see Fig. 6(a) and Fig. 8(a)). Below 300 °C, the coordinated NH<sub>3</sub> reacted with adsorbed NO<sub>2</sub> to form N<sub>2</sub>(L-H mechanism). When the reaction temperature is higher than 300 °C, coordinated NH<sub>3</sub> species reacted with gaseous NO to form nitrite and nitrate which then decomposed to N<sub>2</sub>(E-R mechanism).

Chen et al. [12] found that the addition of tungsten oxide to CeO<sub>2</sub>/TiO<sub>2</sub> catalyst can promote the NO oxidation to NO<sub>2</sub>, which is beneficial for the SCR reaction. In the present study, the addition of Mo to CeO<sub>2</sub>/TiO<sub>2</sub> catalyst does not contribute to the formation of NO<sub>2</sub>, as indicated by the DRIFT spectra in Fig. 6. In comparison with tungsten, the presence of Mo on Ce<sub>10</sub>Mo<sub>5</sub>Ti catalyst is unsaturated. The unsaturated Mo resulted in more Brønsted acid sites formed on the catalyst surface (see Fig. 5(b)), which was favorable for the adsorption of NH<sub>3</sub> thus improving the low-temperature activity [26,29,41]. Anstrom et al. [42] reported a mechanism by using density functional theory calculations that NO reacted with adsorbed NH<sub>4</sub><sup>+</sup> to NH<sub>3</sub>HNO, which reacted further to yield the NH<sub>2</sub>NO. Then the NH<sub>2</sub>NO decomposed to form N<sub>2</sub> and H<sub>2</sub>O. Both the coordinated NH<sub>3</sub> on Lewis acid sites and the NH<sub>4</sub><sup>+</sup> on Brønsted acid sites were considered to be involved in the SCR reaction over Ce<sub>10</sub>Mo<sub>5</sub>Ti catalyst. On one hand, they can react with the adsorbed NO<sub>2</sub>(L-H mechanism), on the other hand, they will react with the gas phase NO (E--R mechanism) followed the reaction route as proposed by Anstrom et al. [42].

In summary, the addition of Mo to Ce<sub>10</sub>Ti catalyst prevents the formation of stable nitrate, leaving more active sites available for the adsorption of NH<sub>3</sub>. Moreover, more Brønsted acid sites formed on the catalyst surface due to the presence of Mo, which appeared to be important for the high SCR activity. Mo also could contribute to the activation of adsorbed NH<sub>3</sub> and NH<sub>4</sub><sup>+</sup>, making them react with NO<sub>x</sub> more easily.

#### 4. Conclusions

CeO<sub>2</sub>-MoO<sub>3</sub>/TiO<sub>2</sub> catalyst is much more active than CeO<sub>2</sub>/TiO<sub>2</sub> for the NH<sub>3</sub>-SCR at relatively low temperatures and the optimum MoO<sub>3</sub> loading is 5%. Based on the in situ DRIFTS studies, it is proposed that the role of MoO<sub>3</sub> is to prevent the formation of stable nitrate species but to promote the formation of Brønsted acid sites, both of which contribute to the adsorption and activation of NH<sub>3</sub> on the catalyst surface, resulting in the higher activity of CeO<sub>2</sub>-MoO<sub>3</sub>/TiO<sub>2</sub> in comparison to CeO<sub>2</sub>/TiO<sub>2</sub>.

#### Acknowledgments

This research was financially supported by the National Natural Science Foundation of China (20907003) and the National

High-tech Research and Development (863) Program of China (2010AA065003).

#### Appendix A. Supplementary data

Supplementary data associated with this article can be found, in the online version, at <http://dx.doi.org/10.1016/j.apcata.2013.06.036>.

#### References

- [1] Z. Liu, J. Hao, L. Fu, T. Zhu, *Appl. Catal. B* 44 (2003) 355–370.
- [2] G. Busca, L. Lietti, G. Ramis, F. Berti, *Appl. Catal. B* 18 (1998) 1–36.
- [3] Z.M. Liu, S.I. Woo, *Catal. Rev. – Sci. Eng.* 48 (2006) 43–89.
- [4] S. Brandenberger, O. Kröcher, A. Tissler, R. Althoff, *Catal. Rev. – Sci. Eng.* 50 (2008) 492–531.
- [5] K. Krishna, G.B.F. Seijger, C.M. Bleek, H.P.A. Calis, *Chem. Commun.* 18 (2002) 2030–2031.
- [6] G. Qi, R.T. Yang, *Chem. Commun.* 7 (2003) 848–849.
- [7] G. Qi, R.T. Yang, R. Chang, *Appl. Catal. B* 51 (2004) 93–106.
- [8] Y. Li, H. Cheng, D.Y. Li, Y.S. Qin, Y.M. Xie, S.D. Wang, *Chem. Commun.* 12 (2008) 1470–1472.
- [9] W.Q. Xu, Y.B. Yu, C.B. Zhang, H. He, *Catal. Commun.* 9 (2008) 1453–1457.
- [10] X. Gao, Y. Jiang, Y.C. Fu, Y. Zhong, Z.Y. Luo, K.F. Cen, *Catal. Commun.* 11 (2010) 465–469.
- [11] P. Li, Y. Xin, Q. Li, Z.P. Wang, Z.L. Zhang, L.R. Zheng, *Environ. Sci. Technol.* 46 (2012) 9600–9605.
- [12] L. Chen, J.H. Li, M.F. Ge, R.H. Zhu, *Catal. Today* 153 (2010) 77–83.
- [13] L. Lietti, P. Forzatti, F. Berti, *Catal. Lett.* 41 (1996) 35–39.
- [14] I. Nova, L. Lietti, L. Casagrandea, L. Dall'Acqua, E. Giamello, P. Forzatti, *Appl. Catal. B* 17 (1998) 245–258.
- [15] L. Lietti, I. Nova, G. Ramis, L. Dall'Acqua, G. Busca, E. Giamello, P. Forzatti, F. Bregani, *J. Catal.* 187 (1999) 419–435.
- [16] L. Casagrande, L. Lietti, I. Nova, P. Forzatti, A. Baiker, *Appl. Catal. B* 22 (1999) 63–77.
- [17] H.L. Koh, H.K. Park, *J. Ind. Eng. Chem.* 19 (2013) 73–79.
- [18] H. Matralis, S. Theret, Ph. Bastians, M. Ruwet, P. Grange, *Appl. Catal. B* 5 (1995) 271–281.
- [19] H. Chen, A. Sayari, A. Adnot, F. Larachi, *Appl. Catal. B* 32 (2001) 195–204.
- [20] A. Trovarelli, G. Dolcetti, C. de Leitenburg, J. Kašpar, P. Finetti, A. Santoni, *J. Chem. Soc., Faraday Trans.* 88 (1992) 1311–1319.
- [21] L.C. Caero, A.R. Romero, J. Ramirez, *Catal. Today* 78 (2003) 513–518.
- [22] M.A. Larrubia, G. Ramis, G. Busca, *Appl. Catal. B* 27 (2000) L145–L151.
- [23] L. Dall'Acqua, I. Nova, L. Lietti, G. Ramis, G. Busca, E. Giamello, *Phys. Chem. Chem. Phys.* 2 (2000) 4991–4998.
- [24] P.G. Smirniotis, D.A. Peña, B.S. Uphade, *Angew. Chem. Int. Ed.* 40 (2001) 2479–2482.
- [25] S.D. Lin, A.C. Gluhoi, B.E. Nieuwenhuys, *Catal. Today* 90 (2004) 3–14.
- [26] L. Chen, J.H. Li, M.F. Ge, *Environ. Sci. Technol.* 44 (2010) 9590–9596.
- [27] Y. Peng, Z.M. Liu, W. Han, J.H. Li, *Catal. Commun.* 19 (2012) 127–131.
- [28] Z.B. Wu, B.Q. Jiang, Y. Liu, H.Q. Wang, R.B. Jin, *Environ. Sci. Technol.* 41 (2007) 5812–5817.
- [29] G. Zhou, B. Zhong, W. Wang, X. Guan, B. Huang, D. Ye, H. Wu, *Catal. Today* 175 (2011) 157–163.
- [30] M. Del Arco, C. Martín, V. Rives, V. Sánchez-Escribano, G. Ramis, G. Busca, V. Lorenzelli, P. Malet, *J. Chem. Soc., Faraday Trans.* 89 (1993) 1071.
- [31] G. Busca, J.C. Lavallee, *Spectrochim. Acta, Part A* 42 (1986) 443–445.
- [32] E. Payen, S. Kasztelan, J. Grimblot, J.P. Bonnelle, *J. Raman Spectrosc.* 17 (1986) 233–241.
- [33] A. Trovarelli, *Catal. Rev. – Sci. Eng.* 38 (1996) 439–520.
- [34] G.M. Underwood, T.M. Miller, V.H. Grassian, *J. Phys. Chem. A* 103 (1999) 6184–6190.
- [35] Y. Chi, S.S.C. Chuang, *Catal. Today* 62 (2000) 303–318.
- [36] J. Valyon, W.K. Hall, *J. Phys. Chem.* 97 (1993) 1204–1212.
- [37] A. Martínez-Arias, J. Soria, J.C. Conesa, X.L. Seoane, A. Arcoya, R. Cataluña, *J. Chem. Soc., Faraday Trans.* 91 (1995) 1679–1687.
- [38] W.S. Kijlstra, D.S. Brands, H.I. Smit, E.K. Poels, A. Bliek, *J. Catal.* 171 (1997) 219–230.
- [39] L. Sun, Q. Cao, B. Hu, J. Li, J. Hao, G. Jing, X. Tang, *Appl. Catal. A* 393 (2011) 323–330.
- [40] G. Qi, R.T. Yang, *J. Catal.* 217 (2003) 434–441.
- [41] Y. Shu, H. Sun, X. Quan, S. Chen, *J. Phys. Chem. C* 116 (2012) 25319–25327.
- [42] M. Anstrom, N.-Y. Topsøe, J.A. Dumesic, *J. Catal.* 213 (2003) 115–125.